PERGAMON

International Journal of Solids and Structures 39 (2002) 5393–5408

INTERNATIONAL JOURNAL OF SOLIDS and STRUCTURES

www.elsevier.com/locate/ijsolstr

An exact transient analysis of plane wave diffraction by a crack in an orthotropic or transversely isotropic solid

L.M. Brock *, M.T. Hanson

Department of Mechanical Engineering, University of Kentucky, 521 CRMS Building Lexington Campus, Lexington, KY 40506-0108, USA

Received 22 November 2000; received in revised form 11 June 2002

Abstract

A transient plane strain analysis of diffraction of plane waves by a semi-infinite crack in an unbounded orthotropic or transversely isotropic solid is performed. The waves approach the crack at a general oblique angle, and are of two types, a normal stress pulse and a shear stress pulse, i.e. a P- and an SV-wave, respectively, in the isotropic limit. A class of materials that includes this limit and beryl, cobalt, ice, magnesium and titanium is chosen for illustration, and exact solutions are obtained for the initial/mixed boundary value problems.

In contrast to related work, a factorization in the Laplace transform space is used to simplify the solution forms and the Wiener-Hopf component of the solution process, and to yield a more compact expression for the Rayleigh wave speed. Calculations for this speed, the two allowable, direction-dependent, plane wave speeds, and quantities related to the Mode I and Mode II dynamic stress intensity factors are given for the five anisotropic materials mentioned.

Keywords: Anisotropy; Crack; Diffraction; Transient problem; Wave propagation; Rayleigh speed

1. Introduction

The study of elastic plane wave diffraction by cracks is a key to understanding both wave scattering (Achenbach, 1973; Miklowitz, 1978) and dynamic fracture (Freund, 1993). As these references attest, plane wave diffraction in cracked isotropic solids is well understood, and the related problem of diffraction by cracks at the welded interfaces of dissimilar isotropic solids has also been addressed (Brock and Achenbach, 1973).

Comprehensive studies of wave propagation in anisotropic solids are available (Kraut, 1963; Scott and Miklowitz, 1967; Payton, 1983), but wave diffraction by cracks has received less attention. Norris and Achenbach (1984) have treated the removal of time-harmonic plane-strain loads by a semi-infinite crack, and Velgaki and Georgiadis (2001) have considered the transient problem of point loads applied to the

* Corresponding author. Tel.: +1-859-257-2839; fax: +1-859-257-8057.
E-mail address: brock@engr.uky.edu (L.M. Brock).

0020-7683/02/$ - see front matter
PII: S0020-7683(02)00355-4

surfaces of a semi-infinite crack. In the present article, therefore, an exact transient plane strain analysis is carried out in a transversely isotropic or orthotropic solid subjected to plane waves impinging on a semi-infinite crack at a largely arbitrary angle. Two types of plane waves are considered: a normal stress pulse that would be a classical dilatational (P-) wave in the isotropic limit, and a shear stress pulse that would be a classical rotational (SV-) wave in the isotropic limit. The pulse forms are largely arbitrary.

Exact solutions are obtained for the two initial/mixed boundary value problems in Laplace transform space by using superposition and the Wiener-Hopf technique (Noble, 1958). The results are inverted for the stresses at small radial distances from the crack edge, and quantities that essentially define the dynamic stress intensity factors are extracted and studied.

For purposes of illustration, a class of orthotropic or transversely isotropic solids that includes beryl, cobalt, ice, magnesium and titanium is examined. Similar classes were treated by Norris and Achenbach (1984), Velgaki and Georgiadis (2001) and, in connection with Lamb's problem, by Payton (1983). Calculations for the intensity factor quantities, and the associated wave speeds and crack plane Rayleigh wave speeds, are given for the five solids mentioned. The two plane wave speeds depend, of course, on the direction of propagation, while a formula, exact to within a simple quadrature, defines the Rayleigh speed.

It should be noted that Velgaki and Georgiadis (2001) followed closely Norris and Achenbach (1984) in the application of the Wiener-Hopf technique and extraction of a crack-plane Rayleigh wave speed. The current study departs from both efforts by employing a factorization that simplifies the solution transform expressions, and removes non-isolated (branch point) singularities that do not occur in the isotropic limt from a function of the Rayleigh type. This procedure allows both a simpler Wiener-Hopf decomposition and a more compact expression for the Rayleigh wave speed.

2. Basic formulation

Consider an unbounded solid containing a crack defined in terms of Cartesian coordinates (x, y, z) as the semi-infinite slit $y = 0, x < 0$. The solid belongs to a class of linear homogeneous anisotropic materials that is governed in plane strain by the field equations

$$c_{11}\frac{\partial^2 u_x}{\partial x^2} + c_{44}\frac{\partial^2 u_x}{\partial y^2} + (c_{13} + c_{44})\frac{\partial^2 u_y}{\partial x\,\partial y} = \rho\ddot{u}_x \tag{1a}$$

$$c_{44}\frac{\partial^2 u_y}{\partial x^2} + c_{33}\frac{\partial^2 u_y}{\partial y^2} + (c_{13} + c_{44})\frac{\partial^2 u_x}{\partial x\,\partial y} = \rho\ddot{u}_y \tag{1b}$$

and the stress–strain formulas

$$\sigma_x = c_{11}\frac{\partial u_x}{\partial x} + c_{13}\frac{\partial u_y}{\partial y} \tag{2a}$$

$$\sigma_y = c_{13}\frac{\partial u_x}{\partial x} + c_{33}\frac{\partial u_y}{\partial y} \tag{2b}$$

$$\sigma_{xy} = \sigma_{yx} = c_{44}\left(\frac{\partial u_y}{\partial x} + \frac{\partial u_x}{\partial y}\right) \tag{2c}$$

These equations hold for both orthotropic and transversely isotropic materials, where the (x, y)-axes are axes of material symmetry. The (u_x, u_y) are the (x, y)-components of displacement, and are functions of (x, y) and time, where $(\cdot)$ denotes time differentiation. The constants $(c_{11}, c_{13}, c_{33}, c_{44})$ are a subset of the elasticities c_{ik} $(i, k = 1, 2, \ldots, 6)$ in the generalized Hooke's law (Sokolnikoff, 1956) and ρ is the mass density. Eqs. (1a) and (1b) follow from generic forms (Scott and Miklowitz, 1967) whose four constants can be linearly related to various subsets of c_{ik}. Overviews of the general relations between c_{ik} and material crystal structure can be found in Nye (1957) and Theocaris and Sokolis (2000). The isotropic limit case can be obtained from (1a), (1b), (2a)–(2c) by setting $c_{11} = c_{33} = \lambda + 2\mu$, $c_{13} = \lambda$ and $c_{44} = \mu$, where (λ, μ) are the Lame' constants (Sokolnikoff, 1956).

For convenience, the dimensionless quantities (Payton, 1983)

$$\alpha = \frac{c_{33}}{c_{44}}, \quad \beta = \frac{c_{11}}{c_{44}}, \quad \gamma = 1 + \alpha\beta - m^2, \quad m = 1 + \frac{c_{13}}{c_{44}} \tag{3}$$

and the temporal variable $s = v_r \times (\text{time})$, where

$$v_r = \sqrt{\frac{c_{44}}{\rho}} \tag{4}$$

are introduced so that the independent variables (x, y, s) all have dimensions of length, and (1a), (1b), (2a), (2b) become, respectively,

$$\left(\beta\frac{\partial^2}{\partial x^2} + \frac{\partial^2}{\partial y^2} - \frac{\partial^2}{\partial s^2}\right)u_x + m\frac{\partial^2 u_y}{\partial x\,\partial y} = 0 \tag{5a}$$

$$\left(\frac{\partial^2}{\partial x^2} + \alpha\frac{\partial^2}{\partial y^2} - \frac{\partial^2}{\partial s^2}\right)u_y + m\frac{\partial^2 u_x}{\partial x\,\partial y} = 0 \tag{5b}$$

$$\frac{1}{c_{44}}\sigma_x = \beta\frac{\partial u_x}{\partial x} + (m-1)\frac{\partial u_y}{\partial y}, \quad \frac{1}{c_{44}}\sigma_y = (m-1)\frac{\partial u_x}{\partial x} + \alpha\frac{\partial u_y}{\partial y} \tag{5c}$$

The quantity defined in (4) is, in the isotropic limit, the classical (Achenbach, 1973) rotational wave speed. For purposes of illustration, the constraints (Payton, 1983)

$$2\sqrt{\alpha\beta} \leqslant \gamma \leqslant 1 + \alpha\beta \quad (1 < \beta < \alpha) \tag{6a}$$

$$\alpha + \beta \leqslant \gamma \leqslant 1 + \alpha\beta \quad (1 < \alpha < \beta) \tag{6b}$$

$$2\alpha \leqslant \gamma \leqslant 1 + \alpha^2 \quad (1 < \beta = \alpha) \tag{6c}$$

are imposed. The class of anisotropic materials governed by (6a)–(6c) includes beryl, cobalt, ice, magnesium and titanium, as well as the isotropic limit.

The solid is at rest when a plane wave is induced which travels toward the crack as depicted schematically in Fig. 1, where $0 < \phi < \pi/2$ gives the attack angle. At $s = 0$ the wavefront reaches the crack edge

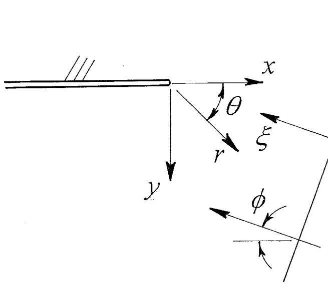

Fig. 1. Schematic of plane wave impinging upon crack.

$(x, y) = 0$, and the ensuing diffraction process generates a transient field in plane strain. Linear superposition allows the total displacement vector $\mathbf{u}$ to be written as

$$\mathbf{u} = \mathbf{u}^{\mathrm{p}} + \mathbf{u}^{\mathrm{s}} + \mathbf{u}^{\mathrm{a}} \tag{7}$$

where $\mathbf{u}^{\mathrm{p}}$ is the incident plane wave field and $(\mathbf{u}^{\mathrm{s}}, \mathbf{u}^{\mathrm{a}})$ are, respectively, the symmetric and anti-symmetric components of the displacement generated by diffraction. The latter two fields can be obtained by studying the half-space $y > 0$. Both fields are governed there by (2c), (5a)–(5c) and the initial conditions

$$\mathbf{u} \equiv 0 \quad (s \leqslant 0) \tag{8}$$

but $\mathbf{u}^{\mathrm{s}}$ satisfies the symmetric mixed boundary conditions

$$\sigma_{yx} = 0; \qquad u_y = 0 \quad (x > 0), \qquad \sigma_y = -\sigma_y^{\mathrm{p}} \quad (x < 0) \tag{9a}$$

on $y = 0$, while $\mathbf{u}^{\mathrm{a}}$ satisfies the anti-symmetric conditions

$$\sigma_y = 0; \qquad u_x = 0 \quad (x > 0), \qquad \sigma_{yx} = -\sigma_{yx}^{\mathrm{p}} \quad (x < 0) \tag{9b}$$

on $y = 0$. In addition, $(\mathbf{u}^{\mathrm{s}}, \mathbf{u}^{\mathrm{a}})$ should be finite for finite $s > 0$, and continuous in $y > 0$, although displacement gradients may exhibit finite discontinuities at wavefronts, and integrable singularities at $(x, y) = 0$.

3. Incident plane wave forms

Consider in light of Fig. 1 the general incident plane wave displacement vector

$$\mathbf{u}^{\mathrm{p}}\left(s + \frac{x}{c}\cos\phi + \frac{y}{c}\sin\phi\right), \quad s + \frac{x}{c}\cos\phi + \frac{y}{c}\sin\phi > 0 \tag{10}$$

in plane strain, where c is a propagation speed non-dimensionalized with respect to v_r.

Substitution into (5a) and (5b) shows that (10) is a valid form only if $c = (c_1, c_2)$ and

$$\frac{u_x^{\mathrm{p}}}{u_y^{\mathrm{p}}} = \frac{m \sin\phi\cos\phi}{c_k^2 - \beta\cos^2\phi - \sin^2\phi} = \frac{c_k^2 - \alpha\sin^2\phi - \cos^2\phi}{m\sin\phi\cos\phi} \quad (k = 1, 2) \tag{11a}$$

$$(c_1^2, c_2^2) = 1 + \frac{\alpha - 1}{2}\sin^2\phi + \frac{\beta - 1}{2}\cos^2\phi \pm \sqrt{\left(\frac{\alpha - 1}{2}\sin^2\phi - \frac{\beta - 1}{2}\cos^2\phi\right)^2 + m^2\sin^2\phi\cos^2\phi} \tag{11b}$$

For $0 < \phi < \pi/2$ and (6a)–(6c), (11b) is positive, i.e. (c_1, c_2) are real-valued. In the isotropic limit, (11b) gives $c_1 = \sqrt{1 + m}$ and $c_2 = 1$, which are the non-dimensionalized speeds of, respectively, dilatational (P-) and rotational (SV-, SH-) waves (Achenbach, 1973).

In view of this behavior, two types of incident waveform are considered: Referring to Fig. 1, type 1 produces the normal stress pulse

$$\sigma_\xi^{\mathrm{p}} = g_1'\left(s + \frac{x}{c_1}\cos\phi + \frac{y}{c_1}\sin\phi\right), \quad s + \frac{x}{c_1}\cos\phi + \frac{y}{c_1}\sin\phi > 0 \tag{12}$$

where g_1 is a bounded, piecewise-continuous function and $(\ )'$ denotes differentiation with respect to the argument. In light of Fig. 1, (2c), (5a)–(5c), (11a), (11b), (12),

$$\left(u_x^{\mathrm{p}}, u_y^{\mathrm{p}}\right) = \left(-\frac{m\cos\phi}{c_{44}\Delta}, \frac{\beta\cos^2\phi + \sin^2\phi - c_1^2}{c_{44}\Delta\sin\phi}\right) c_1 g_1\left(s + \frac{x}{c_1}\cos\phi + \frac{y}{c_1}\sin\phi\right) \tag{13a}$$

$$\left(\sigma_y^{\mathrm{p}}, \sigma_{yx}^{\mathrm{p}}\right) = (e_{\mathrm{I}}, e_{\mathrm{II}}) g_1'\left(s + \frac{x}{c_1}\cos\phi + \frac{y}{c_1}\sin\phi\right) \tag{13b}$$

where, as in (12), the arguments of (g_1, g_1') are positive, and

$$\Delta = \left[(1+m)\cos^2\phi + \alpha\sin^2\phi\right]\left(\beta\cos^2\phi + \sin^2\phi - c_1^2\right) - m\left[(1+m)\sin^2\phi + \beta\cos^2\phi\right]\cos^2\phi \tag{14a}$$

$$\Delta e_{\mathrm{I}} = \alpha\left(\beta\cos^2\phi + \sin^2\phi - c_1^2\right) + m(1-m)\cos^2\phi \tag{14b}$$

$$\Delta e_{\mathrm{II}} = \left(\beta\cos^2\phi + \sin^2\phi - c_1^2 - m\sin^2\phi\right)\cot\phi \tag{14c}$$

Study of (11b) shows that $c_1 = \sqrt{\beta}$ $(\phi = 0)$ and $c_1 = \sqrt{\alpha}$ $(\phi = \pi/2)$, so that the coefficients of (13a) and (13b) are bounded for all $0 < \phi < \pi/2$. In view of this, (12), (13a), (13b) describe in the isotropic limit a classical P-wave.

The type 2 incident plane wave gives, on the other hand, the shear stress pulse

$$\sigma_{\xi\eta}^{\mathrm{p}} = g_2'\left(s + \frac{x}{c_2}\cos\phi + \frac{y}{c_2}\sin\phi\right), \quad s + \frac{x}{c_2}\cos\phi + \frac{y}{c_2}\sin\phi > 0 \tag{15}$$

where g_2 is a bounded, piecewise-continuous function. In this case,

$$\left(u_x^{\mathrm{p}}, u_y^{\mathrm{p}}\right) = \left(\frac{\alpha\sin^2\phi + \cos^2\phi - c_2^2}{c_{44}\Delta\sin\phi}, -\frac{m\cos\phi}{c_{44}\Delta}\right) c_2 g_2\left(s + \frac{x}{c_2}\cos\phi + \frac{y}{c_2}\sin\phi\right) \tag{16a}$$

$$\left(\sigma_y^{\mathrm{p}}, \sigma_{yx}^{\mathrm{p}}\right) = (e_{\mathrm{I}}, e_{\mathrm{II}}) g_2'\left(s + \frac{x}{c_2}\cos\phi + \frac{y}{c_2}\sin\phi\right) \tag{16b}$$

where the arguments are positive, and

$$\Delta = \left[(\beta - m)\cos^2\phi + \sin^2\phi\right]\left(\alpha\sin^2\phi + \cos^2\phi - c_2^2\right) + m\left[(\alpha - m)\sin^2\phi + \cos^2\phi\right]\cos^2\phi \tag{17a}$$

$$\Delta e_{\mathrm{I}} = \left[(m-1)\left(\cos^2\phi - c_2^2\right) - \alpha\sin^2\phi\right]\cot\phi \tag{17b}$$

$$\Delta e_{\mathrm{II}} = c_2^2 + (1-m)\cos^2\phi + \alpha\sin^2\phi \tag{17c}$$

For this wave type, (11b) produces $c_2 = 1$ $(\phi = 0, \pi/2)$; this demonstrates that (15), (16a), (16b) describe a classical SV-wave in the isotropic limit, and that the coefficients in (16a) and (16b) are bounded for $0 < \phi < \pi/2$.

4. Fundamental problem

Consider the same half-space $y > 0$, subject to (2c), (5a)–(5c), (8), but now the unmixed boundary conditions

$$\sigma_y = \sigma(x, s), \quad \sigma_{yx} = \tau(x, s) \tag{18}$$

hold on $y = 0$, where (σ, τ) are no worse than integrably singular, and are bounded for finite $s > 0$. This fundamental problem can be analyzed by introducing the unilateral (Sneddon, 1972) and bilateral (van der Pol and Bremmer, 1950) Laplace transforms

$$\widehat{F} = \int_0^\infty F(s)e^{-ps}\,ds \tag{19a}$$

$$\widetilde{F} = \int_{-\infty}^\infty \hat{F}e^{-pqx}\,dx \tag{19b}$$

and the corresponding inversion operations

$$F = \frac{1}{2\pi i}\int \hat{F}e^{ps}\,dp \tag{20a}$$

$$\widehat{F} = \frac{p}{2\pi i}\int \widetilde{F}e^{pqx}\,dq \tag{20b}$$

Here p is real and positive and large enough to ensure existence of (19a), while q is imaginary. Integration in (20a) and (20b) is over Bromwich contours in, respectively, the p- and q-planes. Application of (19a) and (19b) to (5a), (5b), (8), (18) leads to the transform solutions

$$\tilde{u}_x = U_a e^{-pay} + \left(\alpha b^2 - B^2\right)\frac{U_b}{mqb}e^{-pby} \tag{21a}$$

$$\tilde{u}_y = \left(\alpha a^2 - A^2\right)\frac{U_a}{mq\alpha a}e^{-pay} + U_b e^{-pby} \tag{21b}$$

for $y > 0$, where

$$\frac{c_{44}pR}{mq\alpha a}U_a = -\left[(m-1)B^2 + \alpha b^2\right]q\tilde{\tau} - \left(B^2 - \alpha b^2 + mq^2\right)b\tilde{\sigma} \tag{22a}$$

$$\frac{c_{44}pR}{mqb}U_b = -[(m-1)\alpha a^2 + A^2]q\tilde{\sigma} + (B^2 - \alpha b^2 + mq^2)\alpha a\tilde{\tau} \tag{22b}$$

$$R = \left[(m-1)\alpha a^2 + A^2\right]\left[(m-1)B^2 + \alpha b^2\right]q^2 + \left(B^2 - \alpha b^2 + mq^2\right)^2 AB \tag{22c}$$

In (22a)–(22c) the definitions

$$A = \sqrt{\alpha}\sqrt{1-\beta q^2}, \quad B = \sqrt{1-q^2} \tag{23a}$$

$$\sqrt{2\alpha}(b,a) = \sqrt{S \pm \sqrt{S^2 - 4A^2B^2}} = \frac{1}{\sqrt{2}}\left(\sqrt{S+2AB} \pm \sqrt{S-2AB}\right) \tag{23b}$$

$$S = A^2 + B^2 + m^2q^2 = 1 + \alpha - \gamma q^2, \quad \alpha ab = AB \tag{23c}$$

hold. It can be shown (Payton, 1983) that (6a)–(6c) guarantees that the branch points $q = \pm(1/\sqrt{\beta}, 1)$ of (A, B) lie on the Re(q)-axis, and also constitute branch points of (a, b). Boundedness of (21a) and (21b) requires that $\mathrm{Re}(A, B, a, b) \geqslant 0$ in the cut q-plane. Eq. (23a) also show that $(v_r, \sqrt{\beta}v_r)$ are the speeds of, respectively, rotational and dilatational waves parallel to the x-axis.

Eq. (22c) defines a form of the Rayleigh function. Indeed, in the isotropic limit we have $c_{44} = \mu$, $\alpha = \beta = 1 + m$ and $\gamma = 2(1 + m)$ so that

$$R = m^2(1+m)a_ib_iR_i, \quad R_i = 4q^2a_ib_i + \left(1 - 2q^2\right)^2 \tag{24a}$$

$$a_i = \sqrt{\frac{1}{1+m} - q^2}, \quad b_i = \sqrt{1-q^2} \tag{24b}$$

where R_i is the Rayleigh function for linear isotropic elasticity (Achenbach, 1973). The quantity in (22c) exhibits the isolated real roots $q = \pm 1/c_R$, where $0 < c_R < 1$ and $c_R v_r$ is the speed of Rayleigh waves parallel to the x-axis. The quantity R also vanishes when $b = a$. However, in this limit the exponential terms in (21a) and (21b) are identical, so that these equations become simple linear combinations of $(\tilde{\sigma}, \tilde{\tau})$. It can be shown that the numerators of the resulting coefficients of $(\tilde{\sigma}, \tilde{\tau})$ themselves vanish when $b = a$, so that the additional roots of R play no role in solution behavior.

In the sequel, the displacements along $y = 0$ are required, and so (21a), (21b), (22a)–(22c) are combined to give

$$\tilde{u}_x = \frac{\alpha a N_U}{R} \frac{\tilde{\tau}}{c_{44} p} - \frac{qN}{R} \frac{\tilde{\sigma}}{c_{44} p} \tag{25a}$$

$$\tilde{u}_y = \frac{b N_V}{R} \frac{\tilde{\sigma}}{c_{44} p} + \frac{qN}{R} \frac{\tilde{\tau}}{c_{44} p} \tag{25b}$$

for $y = 0$, where R is given by (22c) and

$$N = \left(A^2 - \alpha a^2\right)\left[(m-1)B^2 + \alpha b^2\right] + \left(B^2 - \alpha b^2 + mq^2\right) mAB \tag{26a}$$

$$N_U = \left(B^2 - \alpha b^2\right)^2 + m^2 q^2 B^2 \tag{26b}$$

$$\alpha b^2 N_V = -A^2 N_U \tag{26c}$$

In the isotropic limit, (25a) and (25b) reduces to forms

$$\tilde{u}_x = -\frac{b_i}{R_i} \frac{\tilde{\tau}}{\mu p} - \frac{N_i}{R_i} \frac{\tilde{\sigma}}{\mu p}, \quad \tilde{u}_y = -\frac{a_i}{R_i} \frac{\tilde{\sigma}}{\mu p} + \frac{N_i}{R_i} \frac{\tilde{\tau}}{\mu p} \tag{27}$$

found for isotropic elasticity (Brock, 1991). Here R_i is given by (24a) and

$$N_i = 2\left(q^2 + a_i b_i\right) - 1 \tag{28}$$

For $y = 0$, the exponential terms in (21a) and (21b) take the same value (unity). Thus, the numerators of the coefficients of $(\tilde{\sigma}, \tilde{\tau})$ in (25a) and (25b) are precisely the ones that vanish when $b = a$. This suggests that simplifications to (25a) and (25b) be made: first, (23b) gives

$$\sqrt{\alpha}(b \pm a) = \sqrt{S \pm 2AB} = \sqrt{(A \pm B)^2 + m^2 q^2} \tag{29}$$

and it follows that $a^2 = b^2$ when $b \pm a = 0$, i.e.

$$q^2 = \frac{\gamma(1+\alpha) - 2\alpha(1+\beta) \pm \mathrm{i}2m\sqrt{\alpha}\sqrt{\gamma - \alpha - \beta}}{\gamma^2 - 4\alpha\beta} \tag{30}$$

In view of (6a)–(6c) the denominator and, in the numerator, the real term and second radical in the imaginary term, are positive and vanish in the isotropic limit. However, the second radical vanishes in this limit as $O(\sqrt{\varepsilon})$, $\varepsilon \to 0$ while the other terms behave as $O(\varepsilon)$, $\varepsilon \to 0$. Therefore, the apparent branch points defined in (30) would move to infinity in the q-plane. Additional cuts for those branch points must be introduced so that the restriction $\mathrm{Re}(a, b) \geqslant 0$ is still met. To this end, $b + a$ is allowed to be continuous across these cuts, although (a, b) themselves are multi-valued. Thus, the additional cuts define branches of $b - a$. Similar situations arose in the studies by Norris and Achenbach (1984) and Velgaki and Georgiadis (2001).

Here, however, we recognize that $b = a$ defines roots of both R and the coefficient numerators in (26a)–(26c) and factor the quantity $b - a$ out of each, thereby canceling them from the formulas. From (A.4), (A.5a), (A.5b) in the Appendix A, and use of (23c), the result

$$\tilde{u}_x = -\frac{\alpha(b+a)B}{2D}\frac{\tilde{\tau}}{c_{44}p} - \frac{Mq}{D}\frac{\tilde{\sigma}}{c_{44}p} \tag{31a}$$

$$\tilde{u}_y = -\frac{(b+a)A}{2D}\frac{\tilde{\sigma}}{c_{44}p} + \frac{Mq}{D}\frac{\tilde{\tau}}{c_{44}p} \tag{31b}$$

for $y = 0$ is obtained, where

$$D = A + \left[A^2 + (m-1)^2 q^2\right]B, \quad M = A + (1-m)B \tag{32}$$

It is noted that, for the restriction (6a)–(6c) the coefficients of $(\tilde{\sigma}, \tilde{\tau})$ exhibit only the branch cuts $\text{Im}(q) = 0$, $|\text{Re}(q)| > 1$ and $\text{Im}(q) = 0$, $|\text{Re}(q)| > 1/\sqrt{\beta}$. In particular, D is analytic in the q-plane cut along $\text{Im}(q) = 0$, $|\text{Re}(q)| > 1/\sqrt{\beta}$ and has the non-isolated real roots $q = \pm 1/c_R$ $(0 < c_R < 1)$. Indeed, setting $D = 0$ and rationalization gives a cubic equation in q^2 that is identical in form to that obtained by Payton (1983) as equation (4.3.22) for the roots of the transversely isotropic Rayleigh function. Thus, D is the essential factor of the Rayleigh function R in (22c) and, as an alternative to the cubic equation, c_R can be found to within a simple quadrature as the formula (B.4a) and (B.4b) in Appendix B. With (31a) and (31b) available, the symmetric and anti-symmetric crack problems for both type 1 and type 2 incident waves can be addressed.

5. Symmetric and anti-symmetric problem solutions

In view of (13b) and (16b), the mixed boundary conditions (9a) for the symmetric problem can be written in the Wiener-Hopf (Noble, 1958) form

$$u_y = \frac{1}{2}V(x,s) \tag{33a}$$

$$\sigma_{yx} = 0 \tag{33b}$$

$$\sigma_y = -e_I g'\left(s + \frac{x}{c}\cos\phi\right)H\left(s + \frac{x}{c}\cos\phi\right)H(-x) + \Sigma(x,s) \tag{33c}$$

for $s > 0$ on $y = 0$. Here $H(\ )$ is the Heaviside function and (13a) and (13b) and (c_1, g_1') are understood for the type 1 incident plane wave, while (16a) and (16b) and (c_2, g_2') are understood for the type 2 case. The function V is the unknown crack-opening displacement, and therefore vanishes identically for $x > 0$ but must be continuous as $x \to 0-$. The function Σ is the unknown normal crack plane stress ahead of the crack, and therefore vanishes for $x < 0$ and may be integrably singular as $x \to 0+$.

The form of (33a)–(33c) implies that the fundamental problem considered above governs the solution to the symmetric problem upon setting $\tau \equiv 0$, equating σ to the right-hand side of (33c) and enforcing the condition (33a). Thus, operating on (33a) and the right-hand side of (33c) with (19a) and (19b) reduces the symmetric problem to the equation

$$\widetilde{V} = -\frac{(b+a)A}{c_{44}pD}\left(\widetilde{\Sigma} - \frac{e_I\hat{g}'}{p(\frac{\cos\phi}{c} - q)}\right) \tag{34}$$

in transform space. Existence requires that $\widetilde{V}$ be analytic for $\mathrm{Re}(q) < \cos\phi/c$ and that $\widetilde{\Sigma}$ and the second term in parentheses be analytic for $\mathrm{Re}(q) > -1/\sqrt{\beta}$ and $\mathrm{Re}(q) < \cos\phi/c$, respectively. The parenthesis coefficient is analytic in the strip $|\mathrm{Re}(q)| < 1/\sqrt{\beta}$, while the singularity in the second term in parentheses is isolated. Therefore, by a standard (Noble, 1958; Achenbach, 1973) process of decomposition by factorization and summation, (34) can be written in a form that equates a term that is analytic for $\mathrm{Re}(q) > -1/\sqrt{\beta}$ to one that is analytic for $\mathrm{Re}(q) < \cos\phi/c$. The key factorization process concerns the quantity $D/(b+a)$ in (34), and is outlined in Appendix B. Because both terms are analytic in the common strip $-1/\sqrt{\beta} < \mathrm{Re}(q) < \cos\phi/c$, they must, by Liouville's theorem, be equal to the same bounded entire function of (p,q). However, continuity of V as $x \to 0-$ requires that $pq\widetilde{V}$ be bounded as $|q| \to \infty$, which implies that the entire function is in fact zero. The result is that two equations exist, and can be solved to yield

$$\widetilde{V} = -\frac{e_{\mathrm{I}}\hat{g}'}{c_{44}p^2}\frac{\sqrt{\gamma + 2\sqrt{\alpha\beta}}}{\alpha\beta - (m-1)^2}\frac{\sqrt{1+\sqrt{\beta}\frac{\cos\phi}{c}}}{\left(\frac{\cos\phi}{c} + \frac{1}{c_R}\right)G_+\left(\frac{\cos\phi}{c}\right)}\frac{\sqrt{1-q\sqrt{\beta}}}{\left(q - \frac{1}{c_R}\right)G_-} \tag{35a}$$

$$\widetilde{\Sigma} = \frac{e_{\mathrm{I}}\hat{g}'}{p\left(\frac{\cos\phi}{c} - q\right)}\left[1 - \frac{\sqrt{1+\sqrt{\beta}\frac{\cos\phi}{c}}}{\sqrt{1+q\sqrt{\beta}}}\frac{q + \frac{1}{c_R}}{\frac{\cos\phi}{c} + \frac{1}{c_R}}\frac{G_+}{G_+\left(\frac{\cos\phi}{c}\right)}\right] \tag{35b}$$

In (35a) and (35b) c_R is defined by (B.4a) and (B.4b) and the terms $G_\pm$ are defined in Appendix B by (B.7a) and (B.7b).

In a similar manner, the mixed condition (9b) for the anti-symmetric case can be treated with the fundamental solution and the Wiener-Hopf approach to give the transform expressions

$$\widetilde{U} = -\frac{e_{\mathrm{II}}\hat{g}'}{c_{44}p^2}\frac{\sqrt{\alpha}\sqrt{\gamma + 2\sqrt{\alpha\beta}}}{\alpha\beta - (m-1)^2}\frac{\sqrt{1+\frac{\cos\phi}{c}}}{\left(\frac{\cos\phi}{c} + \frac{1}{c_R}\right)G_+\left(\frac{\cos\phi}{c}\right)}\frac{\sqrt{1-q}}{(q - \frac{1}{c_R})G_-} \tag{36a}$$

$$\widetilde{T} = \frac{e_{\mathrm{II}}\hat{g}'}{p(\frac{\cos\phi}{c} - q)}\left[1 - \frac{\sqrt{1+\frac{\cos\phi}{c}}}{\sqrt{1+q}}\frac{q + \frac{1}{c_R}}{\frac{\cos\phi}{c} + \frac{1}{c_R}}\frac{G_+}{G_+\left(\frac{\cos\phi}{c}\right)}\right] \tag{36b}$$

Here (T,U) are, respectively, the crack plane shear traction ahead of the crack edge and the crack plane slip. In terms of the fundamental solution, now $\sigma \equiv 0$ and

$$\tau = -e_{\mathrm{II}}g'\left(s + \frac{x}{c}\cos\phi\right)H\left(s + \frac{x}{c}\cos\phi\right)H(-x) + T(x,s) \tag{37}$$

With (35a), (35b), (36a), (36b) and the fundamental solution in hand, the solution process for the symmetric and anti-symmetric problems is essentially complete. The transient behavior of the stresses in the vicinity of the crack generated by diffraction of the two incident waves is now examined.

6. Crack edge transient stress fields

In light of (21a), (21b), (22a)–(22c) superposition and the results obtained above, one can write the transforms of the displacements $(\mathbf{u}^s, \mathbf{u}^a)$ in (7). Operating on (2c) and (5c) with (19a) and (19b) and use of (22a)–(22c) then gives the corresponding stress transforms. Results valid near $(\sqrt{x^2+y^2} \approx 0)$ the crack edge can be obtained by allowing $|q| \to \infty$ and keeping the highest-order terms (van der Pol and Bremmer, 1950). The key step in this operation is use of the asymptotic forms

$$A \approx \sqrt{\alpha\beta}\sqrt{q}\sqrt{-q}, \quad B \approx \sqrt{q}\sqrt{-q}, \quad a \approx a_0\sqrt{q}\sqrt{-q}, \quad b \approx b_0\sqrt{q}\sqrt{-q} \tag{38a}$$

$$a_0 = \frac{1}{2\sqrt{\alpha}}\left(\sqrt{\gamma + 2\sqrt{\alpha\beta}} - \sqrt{\gamma - 2\sqrt{\alpha\beta}}\right), \quad b_0 = \frac{1}{2\sqrt{\alpha}}\left(\sqrt{\gamma + 2\sqrt{\alpha\beta}} + \sqrt{\gamma - 2\sqrt{\alpha\beta}}\right) \tag{38b}$$

where $(a_0, b_0) = 1$ in the isotropic limit, and $\mathrm{Re}(\sqrt{q}, \sqrt{-q}) \geqslant 0$ in planes cut along $\mathrm{Im}(q) = 0$, $\mathrm{Re}(q) < 0$ and $\mathrm{Im}(q) = 0$, $\mathrm{Re}(q) > 0$, respectively. It is then easily shown, for example, that

$$\begin{aligned}\frac{2}{\pi}\tilde{\sigma}_{yx} \approx &-\frac{A_0B_0}{R_0}\sqrt{\alpha}\left(b_0\frac{K_\mathrm{I}}{\sqrt{-q}} + \frac{K_\mathrm{II}}{\sqrt{q}}\right)\frac{\hat{g}'}{p}\mathrm{e}^{-pa_0y\sqrt{q}\sqrt{-q}} \\ &+ \frac{B_0}{R_0}\left(\sqrt{\beta}B_0\frac{K_\mathrm{II}}{\sqrt{q}} + \sqrt{\alpha}b_0A_0\frac{K_\mathrm{I}}{\sqrt{-q}}\right)\frac{\hat{g}'}{p}\mathrm{e}^{-pb_0y\sqrt{q}\sqrt{-q}}\end{aligned} \tag{39}$$

In (39) the definitions

$$A_0 = (m-1)a_0^2 + \beta, \quad B_0 = m - 1 + \alpha b_0^2 \tag{40a}$$

$$R_0 = \sqrt{\gamma - 2\sqrt{\alpha\beta}}\left[\alpha\beta - (m-1)^2\right]\left(\sqrt{\alpha\beta}b_0 - a_0\right) \tag{40b}$$

$$K_\mathrm{I} = \frac{2e_\mathrm{I}}{\pi}\frac{\sqrt{1 + \sqrt{\beta}\frac{\cos\phi}{c}}}{\left(\frac{\cos\phi}{c} + \frac{1}{c_R}\right)\beta^{1/4}G_+\left(\frac{\cos\phi}{c}\right)}, \quad K_\mathrm{II} = \frac{2e_\mathrm{II}}{\pi}\frac{\sqrt{1 + \frac{\cos\phi}{c}}}{\left(\frac{\cos\phi}{c} + \frac{1}{c_R}\right)G_+\left(\frac{\cos\phi}{c}\right)} \tag{40c}$$

hold. In (39) and (40c) the quantities (c_1, g_1') and Eqs. (14a)–(14c) are understood for the type 1 incident plane wave, while (c_2, g_2') and (17a)–(17c) are understood for the type 2 case. It is noted that only the contributions from the diffracted waves appear in (39), because they dominate the stress transform contributions due to the incident waves (12) and (15) themselves for $|q| \to \infty$.

Substitution of the first term in (39) into (20b) gives the two generic inversion operations

$$\frac{\hat{g}'}{2\pi\mathrm{i}}\int \mathrm{e}^{p\left(qx - a_0y\sqrt{q}\sqrt{-q}\right)}\left(\frac{1}{\sqrt{q}}, \frac{1}{\sqrt{-q}}\right)\mathrm{d}q \tag{41}$$

where the Bromwich contour can be taken as the entire Im(q)-axis. Cauchy theory can then be used to change this contour to paths in the q-plane parameterized by

$$q = \frac{-t}{x \pm ia_0y}\,(y > 0) \tag{42}$$

where t is real and positive. Upon introducing the polar coordinates ($r = \sqrt{x^2 + y^2}, \tan\theta = y/x$) depicted in Fig. 1, (41) takes the simple form

$$\frac{\hat{g}'}{\pi\sqrt{r}}(C_a, S_a)\int_0^\infty \frac{\mathrm{e}^{-pt}}{\sqrt{t}}\,\mathrm{d}t \tag{43a}$$

$$C_a = \frac{1}{r_a\sqrt{2r_a}}\left(\cos\theta\sqrt{1 + \frac{\cos\theta}{r_a}} + a_0\sin\theta\sqrt{1 - \frac{\cos\theta}{r_a}}\right) \tag{43b}$$

$$S_a = \frac{1}{r_a\sqrt{2r_a}}\left(\cos\theta\sqrt{1-\frac{\cos\theta}{r_a}} - a_0\sin\theta\sqrt{1+\frac{\cos\theta}{r_a}}\right) \tag{43c}$$

$$r_a = \sqrt{\cos^2\theta + a_0^2\sin^2\theta} \tag{43d}$$

where $r \approx 0$, $0 < \theta < \pi$. In the isotropic limit, $r_a = 1$ and (43b) and (43c) give $(\cos\theta/2, \sin\theta/2)$, respectively. The integration in (43a) gives $\sqrt{\pi/p}$ (Pierce and Foster, 1956). Therefore, the final inversion operation need deal only with the term $\hat{g}'/\sqrt{p}$, and can be performed by inspection and convolution theory (Sneddon, 1972). A similar procedure holds for the transforms of (σ_x, σ_y) as well. In summary, then, the asymptotic results

$$\sigma_x \approx -\left[A_0\left(\sqrt{\beta}B_0C_a + \sqrt{\alpha}D_0C_b\right)K_{\mathrm{I}} + \sqrt{\alpha}a_0B_0(A_0S_a + D_0S_b)K_{\mathrm{II}}\right]\frac{I(s)}{R_0\sqrt{r}} \tag{44a}$$

$$\sigma_y \approx -\left[B_0\left(\sqrt{\beta}C_0 + \sqrt{\alpha}A_0C_b\right)K_{\mathrm{I}} + \sqrt{\alpha}a_0B_0(C_0S_a + B_0S_b)K_{\mathrm{II}}\right]\frac{I(s)}{R_0\sqrt{r}} \tag{44b}$$

$$\sigma_{yx} \approx \left[\sqrt{\alpha}A_0(b_0S_a - S_b)K_{\mathrm{I}} + \left(\sqrt{\beta}B_0C_b - \sqrt{\alpha}A_0C_a\right)K_{\mathrm{II}}\right]\frac{B_0I(s)}{R_0\sqrt{r}} \tag{44c}$$

hold for $s > 0$, $r \approx 0$, $0 < \theta < \pi$, where (C_b, S_b, r_b) follow from (43a)–(43d) by replacing a_0 with b_0, and

$$C_0 = m(m-1) + \alpha(a_0^2 - \beta), D_0 = \beta + [m(m-1) - \alpha\beta]b_0^2 \tag{45a}$$

$$I(s) = \int_0^s \frac{g'(t)}{\sqrt{s-t}}\,\mathrm{d}t \tag{45b}$$

7. Speed and intensity factor behaviors

The speed of Rayleigh waves parallel to the x-axis for the class of anisotropic material considered here is given by c_Rv_r, where (B.4a) and (B.4b) hold. Table 1 presents the dimensionless constant c_R, along with the properties $(\alpha, \beta, m, c_{44})$ for five materials—beryl, cobalt, ice, magnesium and titanium—which satisfy the restriction (6a)–(6c) on this class. The entries show that, as a fraction of the speed v_r, the Rayleigh speeds are similar, and would be typical of isotropic solids (Achenbach, 1973). It should also be noted that the Table 1 data is in agreement with results by Payton (1983).

In Table 2, the dimensionless constants (c_1, c_2) that define the two plane wave speeds supported by the five materials featured in Table 1 are given for various values of attack angle ϕ. It is noted that c_1, which

Table 1
Dimensionless Rayleigh wave speed

	α	β	m	c_{44} (GPa)	c_R
Beryl	3.62	4.11	2.01	68.6	0.956
Cobalt	4.74	4.07	2.37	75.5	0.962
Ice	4.57	4.26	2.64	3.17	0.959
Magnesium	3.74	3.61	2.3	16.4	0.943
Titanium	3.88	3.47	2.48	46.7	0.936

Table 2
Dimensionless plane wave speeds and intensity factors for beryl, cobalt, ice, magnesium, titanium

ϕ	c_1	K_I	K_{II}	c_2	K_I	K_{II}
Beryl						
4.5°	2.025	0.1214	0.0189	1.004	0.099	0.4892
13.5°	2.003	0.1346	0.0576	1.035	0.2771	0.4376
22.5	1.964	0.1637	0.0984	1.086	0.4066	0.3476
31.5°	1.916	0.213	0.14	1.142	0.4782	0.2326
40.5°	1.872	0.2848	0.1737	1.183	0.4937	0.0984
49.5°	1.847	0.3701	0.187	1.19	0.4607	−0.0536
58.5°	1.848	0.4476	0.1715	1.156	0.396	−0.22
67.5°	1.867	0.5032	0.1341	1.098	0.3127	−0.399
76.5°	1.888	0.5394	0.055	1.04	0.2092	−0.5831
85.5°	1.9	0.5641	0.0326	1.005	0.0769	−0.7511
Cobalt						
4.5°	2.016	0.1667	0.0205	1.006	0.1226	0.4878
13.5°	2.001	0.1857	0.0622	1.049	0.3321	0.4214
22.5	1.979	0.2265	0.104	1.119	0.4614	0.313
31.5°	1.96	0.2915	0.1414	1.187	0.5083	0.1848
40.5°	1.962	0.3736	0.1631	1.225	0.491	0.0456
49.5°	1.994	0.4505	0.1597	1.2167	0.4357	−0.1014
58.5°	2.048	0.504	0.1351	1.168	0.3664	−0.2559
67.5°	2.104	0.5394	0.1002	1.102	0.2887	−0.4209
76.5	2.149	0.5532	0.0619	1.041	0.1937	−0.5936
85.5°	2.174	0.5683	0.0215	1.005	0.0713	−0.7536
Ice						
4.5°	2.062	0.19	0.0202	1.004	0.1079	0.4891
13.5°	2.05	0.2065	0.0605	1.037	0.2971	0.4286
22.5°	2.029	0.2413	0.1001	1.0896	0.4239	0.326
31.5°	2.01	0.2947	0.1348	1.142	0.4823	0.2004
40.5°	2.003	0.3617	0.1566	1.174	0.4837	0.0613
49.5°	2.017	0.4289	0.1579	1.171	0.4458	−0.0881
58.5°	2.048	0.4828	0.1389	1.136	0.385	−0.25
67.5°	2.086	0.52	0.1067	1.084	0.3066	−0.419
76.5°	2.118	0.5447	0.068	1.034	0.2057	−0.595
85.5°	2.135	0.5631	0.024	1.004	0.0754	−0.7556
Magnesium						
4.5°	1.899	0.1743	0.0236	1.002	0.0861	0.481
13.5°	1.892	0.1904	0.07	1.018	0.2439	0.4296
22.5	1.881	0.223	0.1135	1.045	0.3646	0.3367
31.5°	1.87	0.1713	0.1498	1.071	0.438	0.2138
40.5°	1.866	0.3313	0.1724	1.088	0.4644	0.0757
49.5°	1.872	0.3944	0.176	1.087	0.4504	−0.0864
58.5°	1.887	0.4515	0.1589	1.07	0.403	−0.2522
67.5°	1.91	0.4972	0.1259	1.043	0.3255	−0.4211
76.5°	1.923	0.5315	0.0817	1.0716	0.2176	−0.5838
85.5°	1.933	0.5564	0.0291	1.002	0.0791	−0.7241
Titanium						
4.5°	1.863	0.2046	0.0257	1.001	0.0792	0.4773
13.5°	1.863	0.2213	0.0751	1.01	0.2264	0.4267
22.5	1.867	0.2537	0.1185	1.024	0.3434	0.3328
31.5°	1.872	0.2988	0.151	1.037	0.42	0.2067
40.5°	1.884	0.3516	0.1684	1.045	0.4542	0.0589
49.5°	1.902	0.4054	0.1681	1.044	0.4484	−0.0108

Table 2 (*continued*)

ϕ	c_1	K_I	K_{II}	c_2	K_I	K_{II}
58.5°	1.923	0.4545	0.151	1.035	0.4061	−0.2679
67.5°	1.943	0.4956	0.12	1.021	0.3294	−0.4319
76.5	1.96	0.528	0.0782	1.009	0.2196	−0.5884
85.5°	1.969	0.552	0.0279	1.001	0.0795	−0.7136

corresponds to a dilatational (P-) wave speed in the isotropic limit, achieves maximum values for $\phi = (0, \pi/2)$. The opposite effect occurs for c_2, which corresponds in the isotropic limit to a rotational (SV-) wave speed. Indeed, its maximum value occurs roughly in the mid-range of ϕ, and is nearly 20% higher than its limit values at $\phi = (0, \pi/2)$. Thus, a type 1 plane wave loses speed by traveling at angles to the material symmetry (x-, y-) axes of the solids considered here, while the type 2 wave gains speed. These results are also consistent with the studies by Payton (1983) and Norris and Achenbach (1984).

Eq. (45b) shows that $I(s)$ is merely a weighted history of the plane wave stress pulse functions (g_1', g_2'). In view of (40c), (44a)–(44c), therefore, it is the dimensionless quantities (K_I, K_{II}) that essentially define, respectively, the Modes I and II dynamic stress intensity factors for the diffraction process. Values for these quantities are, therefore, given in Table 2 for the type 1 and type 2 plane wave cases. The data indicates behavior similar to that for their respective (P-wave, SV-wave) isotropic limit cases: For type 1, K_I increases with ϕ, while K_{II} reaches a maximum in the mid-range of $0 < \phi < \pi/2$. Moreover, the maximum values of K_I are much larger than those of K_{II}. For type 2, on the other hand, K_I achieves a mid-range maximum, while K_{II} changes sign in mid-range, and the maximum values are more comparable.

Thus, a stress intensity factor-based fracture criterion (Freund, 1993) might predict failure for type 1 plane waves that approach the crack at a single oblique angle, while two such angles might arise for type 2 plane wave diffraction.

8. Comments

This article considered the transient plane-strain problem of diffraction of plane waves by a semi-infinite crack in an unbounded orthotropic or transversely isotropic solid. A class of materials that included beryl, cobalt, ice, magnesium and titanium was chosen for illustration, the plane waves approached the crack at a general oblique angle of attack, and were of two types. One type was a normal traction pulse that reduced to a classical dilatational (P-) wave in the isotropic limit, and the other, a shear traction pulse that reduced to a rotational (SV-) wave.

Linear superposition and symmetry arguments reduced the analysis to the treatment of initial/mixed boundary value problems, solved by Laplace transform and Wiener-Hopf techniques. An exact solution in the transform space was obtained, and expressions for all stresses at small radial distances from the crack edge were obtained by inversion.

The incident plane wave pulses were largely arbitrary, and it was found that two dimensionless quantities essentially defined the Modes I and II dynamic stress intensity factors for any pulse form. Values of these quantities at various attack angles were given for the five materials noted above. Their variation with angle was similar to that for diffraction of P- and SV-waves in an isotropic solid.

The speeds of plane wave propagation also varied with attack angle, and exact formulas for those speeds gave values at various angles for the five materials. These showed that the speed of the normal traction pulse was maximized when wave travel was parallel to a material symmetry axis, while the speed of the shear traction pulse reached a maximum when propagation was at an oblique angle. Such behavior was consistent with previous studies in anisotropic solids. Calculations based on a formula (Appendix B), analytic to within a simple quadrature, showed for the five materials that the values of the crack plane Rayleigh wave speed were similar to those for isotropic solids.

In summary, transient studies of wave diffraction by cracks (and the possibility of dynamic fracture) in anisotropic solids do yield results that show both the importance of anisotropy, but also the similarities in behavior with studies in isotropic solids. Indeed, manipulations in the transform space can partly offset the complications that arise in the treatment of anisotropic solids.

Acknowledgements

This work was aided by discussions on anisotropy with Dr. H.G. Georgiadis of the National Technical University of Athens, during his leave at the University of Kentucky. It is inspired by the contributions of J.D. Achenbach to the study of dynamic fracture.

Appendix A

Consider N_V defined by (26c). By using (26b) and (23c), it can be written as

$$N_V = (B^2 - \alpha b^2)(A^2 - \alpha a^2) - m^2 q^2 \alpha a^2 \tag{A.1}$$

Carrying out the multiplication and using (23a), (23b), (29) gives

$$N_V = 2A^2B^2 - \frac{S^2}{2} + \frac{\alpha^2}{2}(b^2 - a^2)^2 (m^2 q^2 + B^2 - A^2) \tag{A.2}$$

But (23a), (23b), (29) also show that

$$S^2 - 4A^2B^2 = \alpha^2 (b^2 - a^2)^2, \quad m^2 q^2 + B^2 = \frac{\alpha}{2}(b + a + b - a) - A^2 \tag{A.3}$$

whereupon (A.2) and N_U given by (26b) can be written as

$$N_V = \alpha(b^2 - a^2)(\alpha a^2 - A^2), \quad N_U = \left(\frac{\alpha b}{A}\right)^2 (b^2 - a^2)(\alpha a^2 - A^2) \tag{A.4}$$

In similar fashion, (26a) and (22c) can be written as

$$N = \frac{B}{a}(b - a)(A^2 - \alpha a^2)M, \quad M = A + (1 - m)B \tag{A.5a}$$

$$R = \frac{B}{a}(b - a)(A^2 - \alpha a^2)D, \quad D = A + \left[A^2 + (m - 1)^2 q^2\right]B \tag{A.5b}$$

These functions all exhibit the common factor $(b - a)(A^2 - \alpha a^2)$.

Similar factorizations of the terms (R_i, N_i) in (24a) and (28) that arise in the isotropic limit can also be performed:

$$N_i = (b_i - a_i)\left(\frac{1 + m}{m} a_i + \frac{1 - m}{m} b_i\right) \tag{A.6a}$$

$$R_i = \frac{2}{m}(b_i - a_i)\left[(1 + m)a_i + (1 + m - 4q^2)b_i\right] \tag{A.6b}$$

Appendix B

From (32) consider the function D/A. It exhibits the branch cuts $\mathrm{Im}(q) = 0, 1/\sqrt{\beta} < |\mathrm{Re}(q)| < 1$, has the isolated real roots $q = \pm 1/c_R$ $(0 < c_R < 1)$ and behaves as

$$\left[\frac{(m-1)^2}{\sqrt{\alpha\beta}} - \sqrt{\alpha\beta}\right] q^2, \quad |q| \to \infty \tag{B.1}$$

We define, therefore, the function

$$F = \frac{D\sqrt{\alpha\beta}}{A\left[\alpha\beta - (m-1)^2\right]} \frac{1}{\frac{1}{c_R^2} - q^2} \tag{B.2}$$

that is analytic in the same cut plane, but has no roots there, and behaves as unity when $|q| \to \infty$. This function can be written as the product of two functions, $F_\pm$, that are analytic in the overlapping regions $\mathrm{Re}(q) > -1/\sqrt{\beta}$ and $\mathrm{Re}(q) < 1/\sqrt{\beta}$, respectively, by means of a standard procedure (Noble, 1958), where

$$\ln F_\pm = \frac{1}{\pi} \int_{1/\sqrt{\beta}}^{1} \frac{\omega \, \mathrm{d}t}{t \pm q} \tag{B.3a}$$

$$\omega = \tan^{-1} \frac{\sqrt{1-t^2}}{\sqrt{\alpha}\sqrt{\beta t^2 - 1}} \left[\alpha + ((m-1)^2 - \alpha\beta)t^2\right] \tag{B.3b}$$

Both $F_\pm$ are analytic in the common strip $|\mathrm{Re}(q)| < 1/\sqrt{\beta}$, and (B.2) holds there as well. Therefore, setting $q = 0$ in (B.2) and using (B.3a) and (B.3b) gives the formula

$$c_R = \sqrt{\frac{\alpha\beta - (m-1)^2}{(1+\sqrt{\alpha})\sqrt{\alpha\beta}} F_R} \tag{B.4a}$$

$$\ln F_R = \frac{1}{\pi} \int_{1/\sqrt{\beta}}^{1} \frac{\omega \, \mathrm{d}t}{t} \tag{B.4b}$$

Here (6a)–(6c) guarantees that the coefficient of F_R is real and positive. A similar approach was used by Norris and Achenbach (1984), albeit for a more complicated function than D/A. Some other examples for this root-finding approach are given by Brock (1998).

Now consider from (34) the function $D/\sqrt{\alpha}(b+a)$. It exhibits the same branch cuts and isolated roots as does D/A, but behaves as

$$\frac{(m-1)^2 - \alpha\beta}{\sqrt{\gamma + 2\sqrt{\alpha\beta}}} q^2, \quad |q| \to \infty \tag{B.5}$$

The function

$$G = \frac{D}{\sqrt{\alpha}(b+a)} \frac{\sqrt{\gamma + 2\sqrt{\alpha\beta}}}{\alpha\beta - (m-1)^2} \frac{1}{\frac{1}{c_R^2} - q^2} \tag{B.6}$$

is defined, where (6a)–(6c) guarantees that the central ratio is real and positive. This function can also be written as the product of two functions, $G_\pm$, that are analytic in the same overlapping regions as were, respectively, $F_\pm$. In this case, the standard procedure (Noble, 1958) yields

$$\ln G_{\pm} = -\frac{1}{\pi}\int_{1/\sqrt{\beta}}^{1} \frac{\Omega\,\mathrm{d}t}{t \pm q} \tag{B.7a}$$

$$\Omega = \tan^{-1} \frac{\sqrt{\alpha}\sqrt{\beta t^2 - 1}}{B} \frac{\alpha b^2 - B^2\left[A^2 + (m-1)^2 t^2\right]}{\alpha b^2\left[A^2 + (m-1)^2 t^2\right] - A^2} \tag{B.7b}$$

where $(-A^2, B, b)$ are defined in (23a) and (23b), with t replacing q, and it is noted that these quantities are real and positive for $1/\sqrt{\beta} < t < 1$. In the isotropic limit, (B.7b) appropriately reduces to (Achenbach, 1973)

$$\Omega = \tan^{-1} \frac{4t^2\sqrt{1-t^2}\sqrt{t^2 - \frac{1}{1+m}}}{(1-2t^2)^2} \tag{B.8}$$

It should be noted that an expression for c_R could also be obtained by setting $q = 0$ in (B.6) and using (B.7a). The integrand term Ω is more complicated than its counterpart ω in (B.4b), however, so that the formula is less compact.

References

Achenbach, J.D., 1973. Wave Propagation in Elastic Solids. North-Holland, Amsterdam.

Brock, L.M., 1991. Exact transient results for pure and grazing indentation with friction. Journal of Elasticity 33, 119–143.

Brock, L.M., 1998. Analytical results for roots of two irrational functions in elastic wave propagation. Journal of the Australian Mathematical Society B 40, 72–79.

Brock, L.M., Achenbach, J.D., 1973. Extension of an interface flaw under the influence of transient waves. International Journal of Solids and Structures 9, 53–68.

Freund, L.B., 1993. Dynamic Fracture Mechanics. Cambridge University Press, Cambridge.

Kraut, E.A., 1963. Advances in the theory of anisotropic wave propagation. Reviews of Geophysics 1, 401–488.

Miklowitz, J., 1978. The Theory of Elastic Waves and Waveguides. North-Holland, Amsterdam.

Noble, B., 1958. Methods Based on the Wiener-Hopf Technique. Pergamon, New York.

Norris, A.N., Achenbach, J.D., 1984. Elastic wave diffraction by a semi-infinite crack in a transversely isotropic material. Quarterly Journal of Mechanics and Applied Mathematics 14, 293–317.

Nye, J.F., 1957. Physical Properties of Crystals, Their Representation by Tensors and Matrices. Clarendon Press, Oxford.

Payton, R.G., 1983. Elastic Wave Propagation in Transversely Isotropic Media. Martinus Nijhoff, The Hague.

Pierce, B.O., Foster, R.M., 1956. A Short Table of Integrals, fourth ed. Blaisdell, Waltham, MA.

Scott, R.A., Miklowitz, J., 1967. Transient elastic waves in anisotropic plates. ASME Journal of Applied Mechanics 34, 104–110.

Sneddon, I.N., 1972. The Use of Integral Transforms. McGraw-Hill, New York.

Sokolnikoff, I.S., 1956. Mathematical Theory of Elasticity, second ed. McGraw-Hill, New York.

Theocaris, P.S., Sokolis, D.P., 2000. Invariant elastic constants and eigentensors of orthorhombic, tetragonal, hexagonal and cubic crystalline media. Acta Crystallographica A 56, 319–331.

van der Pol, B., Bremmer, H., 1950. Operational Calculus Based on the two-Sided Laplace Integral. Cambridge University Press, Cambridge.

Velgaki, E.G., Georgiadis, H.G., 2001. Elastodynamic response of a cracked fiber-reinforced body to a non-uniform plane-strain loading. Proceedings of the IUTAM Symposium on Mechanical Waves for Composite Structures Characterization (Sotiropoulos, D.A., ed.) Kluwer, Dordrecht.